



The anhysteretic polarisation of ferroelectrics

B Kaeswurm^{1,3}, V Segouin², L Daniel² and K G Webber¹

¹ Materials Science and Engineering Department, Friedrich-Alexander-Universität Erlangen-Nürnberg, 91058 Erlangen, Germany

² Group of Electrical Engineering Paris (GeePs) UMR CNRS 8507, CentraleSupélec, Univ. Paris-Sud, Université Paris-Saclay, Sorbonne Universités, UPMC Univ. Paris 06 3 & 11 rue Joliot-Curie, Plateau de Moulon 91192 Gif-sur-Yvette CEDEX, Paris, France

E-mail: barbara.kaeswurm@fau.de

Received 30 October 2017, revised 2 January 2018

Accepted for publication 10 January 2018

Published 30 January 2018




CrossMark

Abstract

Measurement and calculation of anhysteretic curves is a well-established method in the field of magnetic materials and is applied to ferroelectric materials here. The anhysteretic curve is linked to a stable equilibrium state in the domain structure, and ignores dissipative effects related to mechanisms such as domain wall pinning. In this study, an experimental method for characterising the anhysteretic behaviour of ferroelectrics is presented, which is subsequently used to determine the anhysteretic polarisation response of polycrystalline barium titanate and a doped lead zirconate titanate composition at room temperature. Various external parameters, such as electric field, stress, and temperature, can significantly affect ferroelectric behaviour. Ferroelectric hysteresis curves can assess the importance of such effects but cannot distinguish their contribution on the different intrinsic and extrinsic mechanisms involved in ferroelectric behaviour. In this work, the influence of compressive stress on the anhysteretic polarisation is measured and discussed. The comparison of the polarization loop to the anhysteretic curve under compressive stress elucidates the effects on the stable equilibrium domain configuration and dynamic effects associated to dissipation.

Keywords: ferroic, hysteresis, anhysteretic polarisation, ferroelectric, barium titanate, lead zirconate titanate

 Supplementary material for this article is available [online](#)

(Some figures may appear in colour only in the online journal)

1. Introduction

Below their Curie temperature, ferroic materials show a dependence of the order parameter, not only on the external field experienced at the point of the measurement, but also on the previously experienced field and thermal history. The dependence of the dielectric displacement, D or polarisation, P on the electric field E in ferroelectric materials show similarities to the dependence of the magnetic induction, B or magnetization, M on the magnetic field H in magnetic materials. The order parameter (D , P , B or M) versus field (E or H) measurement is a double-valued hysteresis loop

[1–4]. Starting from an initially demagnetized or depolarized state and increasing the field strength, the ordering parameter follows the ‘virgin’ or ‘initial’ curve. At large applied field values, the magnetic moments or electric dipoles align as closely to the field vector as allowed by the system. In this state, the material has reached so-called ‘technical saturation’. In the case of ferromagnetic materials, further increase in the magnetic field leads to negligible increase in magnetization. For ferroelectric materials, the situation is more complex, as electrical conductivity can lead to an increase in the apparent polarisation and possible misinterpretation [5–10] as well as dielectric breakdown. When the field is reduced, the values for the ordering parameter follow a different path. The new value at zero field is called remanence and the field needs to

³ Author to whom any correspondence should be addressed.

be reduced until the coercive field, or coercivity, at zero M or P is measured. When saturation is reached in both the positive and negative field directions, the hysteresis loop is referred to as a ‘major hysteresis loop’.

When the field is not increased to saturation but reversed at an intermediate point, the hysteresis loop is referred to as a ‘minor loop’. While there is some evidence of repeatability within the ferromagnetic domain structure after field cycling below saturation observed by magnetic force microscopy [11], the minor M – H curve, which averages over the domains of the entire sample are strongly history dependent. Minor M – H curves are reported when they resemble the working field of a practical application [12–14]. Experimentally obtained ferroelectric minor hysteresis loops of polycrystalline $\text{Pb}(\text{Zr},\text{Ti})\text{O}_3$ (PZT) have been reported in the context of the Preisach model of hysteresis [15] and nucleation-growth model of ferroelectric switching based on the Gibbs–Landau–Devonshire theory [16]. There are a number of different measurement protocols where the field is applied and reversed in a controlled fashion, while not reaching saturation on both sides of the loop. This is done to determine specific material parameters for practical applications. For example, intergranular interactions and intrinsic switching fields have been measured in magnetic recording media using measurement protocols such as δM [17]. This has allowed the materials used to be tailored to improve the stability of recorded information.

Another example is the first order reversal curve (FORC), where the field is ramped down from saturation to a reversal field and then increased back to saturation [18–20]. Ferroelectric FORC diagrams have been used to study ferroelectric switching in PZT [21, 22] and Nb-doped PZT [23]. The dependence of dielectric constant on grain size in BaTiO_3 (BT) [24] as well as the film thickness dependence in PZT [25] has also been studied using FORC.

A measure of how a material would respond in the absence of hysteresis is given by the ‘ideal curve’ or ‘anhysteretic curve’. ‘Anhysteresis’ is the antonym of ‘hysteresis’ and refers to independence of measurement history and independence of the effects of defects or dissipation. The magnetic anhysteretic curve is a well-established concept for ferromagnetic materials [1–3]. The anhysteretic curve is used as a simplifying approach to deal with the complexity of real materials. Measurements and calculations of the anhysteretic curve have been reported for wide range of materials, such as multiphase alloys [26], fine particles [27], permanent magnets [28], magnetic tapes [29, 30], and polycrystalline electrical steels [31]. In audio recording, the anhysteretic curve was of great interest due to the near linear dependence at low fields [2]. In analogue recording it was required to linearize the response of the medium to the field in the recording head and, hence, the current in the recording head, which related to the signal amplitude. This is no longer necessary. The anhysteretic curve can be used to study internal stress in bulk [32–34]. It is also widely used for numerical modelling of electromagnetic devices, where the material constitutive laws are often limited to the reversible contribution, allowing robust computational schemes. The dissipative contribution can then be evaluated using so-called ‘*a posteriori* approaches’ [35]. The reversible

part is linked to the energetic equilibrium in the domain structure, while the dissipative part is related to a meta-stable equilibrium linked to the presence of defects causing domain wall pinning [36]. Using a similar approach, the anhysteretic curve has been proposed for numerical modelling of ferroelectric materials [37, 38].

The anhysteretic curve cannot be obtained continuously by applying a monotonically increasing field. For magnetic materials there are several methods to obtain the anhysteretic curve, which lead to slightly different results, especially at very low fields. It is not possible to remove defects from a material, but it is possible to follow a measurement procedure in which the dipoles are disordered in such a way so as to overcome frictional forces and switching effects in order to reach a true equilibrium value. This can be brought about by a magnetic/electric field, stress, or temperature. In one method, a constant unidirectional field is superimposed with a decaying alternating field. The alternating field starts at an amplitude saturating the material and is slowly decreased until only the unidirectional bias field remains. This procedure is then repeated for different constant unidirectional fields, referred to as bias fields [1–3]. Sometimes, the anhysteretic curve is replaced by a single-valued curve determined by measuring a number of symmetrical minor loops with decreasing applied field and connecting the tips of the loops [3]. This is not an anhysteretic curve, in the sense that each data point does not correspond to the equilibrium state of the material. An anhysteretic curve can also be obtained by cooling the sample from above the Curie temperature down to the measurement temperature with an applied external field [2, 39]. This is similar to the well-known thermoremanent magnetization measurement protocol (TRM), with the difference being that here the magnetization is obtained at the bias field, not at remanence as in TRM. Sometimes the anhysteretic remanent magnetization (ARM) is reported. In this case, the bias field is removed after the usual anhysteretic treatment before the value is recorded [28, 29, 40, 41]. The initial slope is referred to as the ARM susceptibility and has a magnitude greater than the conventional initial susceptibility [2]. The anhysteretic curve for magnetic materials is independent of the parameters such as period, time, and amplitude, as long as the amplitude is above the amplitude for technical saturation, the frequency of the signals sufficiently low, and the waveform sufficiently smooth.

One of the mechanisms contributing to hysteresis is the impediment of domain movement by defects, referred to as domain wall pinning. The pinning depends on the type of defect, its size and location. There are, however, some major physical differences between ferromagnetic and ferroelectric materials. In ferromagnetic materials hysteresis is largely a consequence of imperfections in the material since short distance disturbances due to defects have a major influence to the exchange interaction and RKKY (Ruderman–Kittel–Kasuya–Yosida) interaction [1–3]. Since the Coulomb interaction is less sensitive to short distance changes compared to the exchange and RKKY interactions, the influence of defects plays a less prominent role in ferroelectric materials and the intrinsic contribution due to non-centrosymmetric crystals

structure is the larger contribution. The interplay between domain walls and defects and the overall appearance of the ferroelectric hysteresis is still not precisely known. Defect dipoles and free charges contribute to the measured polarization as well as interact with domain walls. The main aim of this work is to introduce the concept of the anhysteretic polarization curve and to demonstrate that it can be obtained experimentally for well-known ferroelectrics.

2. Experimental method

In this work, the anhysteretic polarisation of polycrystalline BaTiO₃ (BT) and Pb(Zr,Ti)O₃ (PZT) was characterized at room temperature. BT samples were prepared from commercially available powder (99% Sigma Aldrich) which was milled for 3 h in ethanol using zirconia milling balls, uniaxially compacted into disk shape and then cold-isostatically-pressed. The compacted samples were sintered at 1300 °C for 4 h and then ground to the required dimensions. The PZT material used here is the commercially available composition Pb_{0.99}(ZrTi_{0.47}(Sb_{0.67}Nb_{0.33})_{0.08})O₃ (PIC 151, PI Ceramics), which is electrically and mechanically ‘soft’ and hereafter referred to as ‘doped PZT’. The crystal structure of the samples was confirmed by x-ray diffraction and the data is available as supplementary information (stacks.iop.org/JPhysD/51/075305/mmedia). For electrical measurements, samples of thickness of 1 mm were used, whereas measurements under mechanical stress were conducted on a cylindrical sample with a diameter of 5.8 mm and a height of 6 mm. Before measurement, the samples were annealed at 600 °C to remove residual stresses and measurement history. During electrical measurement the samples were placed in an insulating oil to prevent dielectric breakdown. A voltage $V(t)$ was applied to the sample by a high voltage amplifier (Trek 20/20C), to obtain an electric field $E(t)$ following equation (1):

$$E(t) = E_A \sin(\omega t) \exp(-k\omega t) + E_B [1 - \exp(-k\omega t)] \quad (1)$$

where $\omega = 2\pi f$ and f is the frequency, E_A is the initial electric field amplitude, k is a damping factor, and E_B the bias field. The input signal to the high voltage amplifier as well as the data acquisition and analysis were realized using a LabVIEW program. The polarisation was measured using a Sawyer-Tower circuit with a reference capacitor of 4.65 nF. Electrical measurements under mechanical stress were conducted using a screw-driven load frame (Zwick/Roell Z030) with a sample loading die and oil bath. Here, a Sawyer-Tower circuit with a reference capacitor of 9.7 nF was used.

3. Results and discussion

Figure 1 shows the details of how the anhysteretic curve was obtained for doped PZT using a maximum field of $E_A = 40 \text{ kV cm}^{-1}$, a damping factor of $k = 0.015$, and a frequency of 0.5 Hz. It was found that a larger damping factor and, hence, more rapid decay did not allow for the frictional forces and switching fields to be overcome, resulting in low measurement repeatability. In contrast, a smaller damping factor unnecessarily

increased the measurement time. As shown in figure 1(a), the polarisation decays rapidly to a value of zero as the electric field amplitude decreases ($E_B = 0$), corresponding to a field depolarisation. This was also observed in the macroscopic P - E loops (figure 1(b)), which show the initial development of a remanent polarisation, followed by a subsequent decay of the remanent polarisation to zero with gradually smaller electric field amplitude. In contrast, figures 1(c) and (d) show the influence of a bias electric field ($E_B = 20 \text{ kV cm}^{-1}$), where the final polarisation value obtained after all frictional forces and switching fields are overcome corresponds to the equilibrium state for this particular bias field. This final polarisation value was determined for various bias electric field values, allowing for the construction of an anhysteretic curve (figure 2(a)). It is important to note that at high bias fields conduction can play an increasing role, necessitating the reduction in measurement time after which the equilibrium value can be recorded.

Figures 2(a) and (b) show anhysteretic polarisation curves compared to representative major hysteresis loops for BT and doped PZT, respectively. The anhysteretic curve lies within the major loop and approaches it at high fields. The anhysteretic curve corresponds to the domain wall positions of true equilibrium at a given electric field. At low fields, the polarisation switching is strongly affected by domain wall motion, which is impeded by pinning and bowing of the domain walls at defects [42–48] and also depends on the crystallographic direction [49]. The pinning depends on the size, type, and location of the defects. The ferroelectric defect dipoles and free charges contribute to the polarisation that is measured and also interact with the domain walls [50]. The anhysteretic curve, which is a measure of the equilibrium state, therefore, differs most from the non-equilibrium major curve at low fields. At high fields, the hysteresis loop and the anhysteretic curve both become more similar to the virgin curve. This is the saturation region, where the reversal mechanism is least dominated by defects. For BT, the initial anhysteretic susceptibility, defined as the slope of the anhysteretic curve at very low fields, is twice as large as the conventional initial susceptibility. For the doped PZT sample, there is a factor 10 difference between the equilibrium and non-equilibrium susceptibility. The doped PZT composition of the commercially available sample studied here is one where the properties are largely governed by its dopants, which can result in an increased concentration of lattice defects. Due to the lower coercivity of BT, changes are less visible in this material. Since the difference between the anhysteretic polarisation and major loop is more prominent in doped PZT than in BT, stress dependent measurements are presented for the doped PZT only.

Figure 3 shows the influence of a uniaxial compressive stress on the anhysteretic and depolarisation curves of doped PZT. It is clear that in this case the anhysteretic curve cannot be produced by linking up the tips of the ‘minor hysteresis loops’. The measurements were obtained at $f = 0.1 \text{ Hz}$. From comparison of the major loops obtained at 5 MPa in figure 3(a) and 50 MPa shown in figure 3(b), it is clear that application of compressive stress, for a given level of maximum electric field, reduces the level of hysteresis. A reduction in hysteresis under high stress has been observed in lanthanum doped

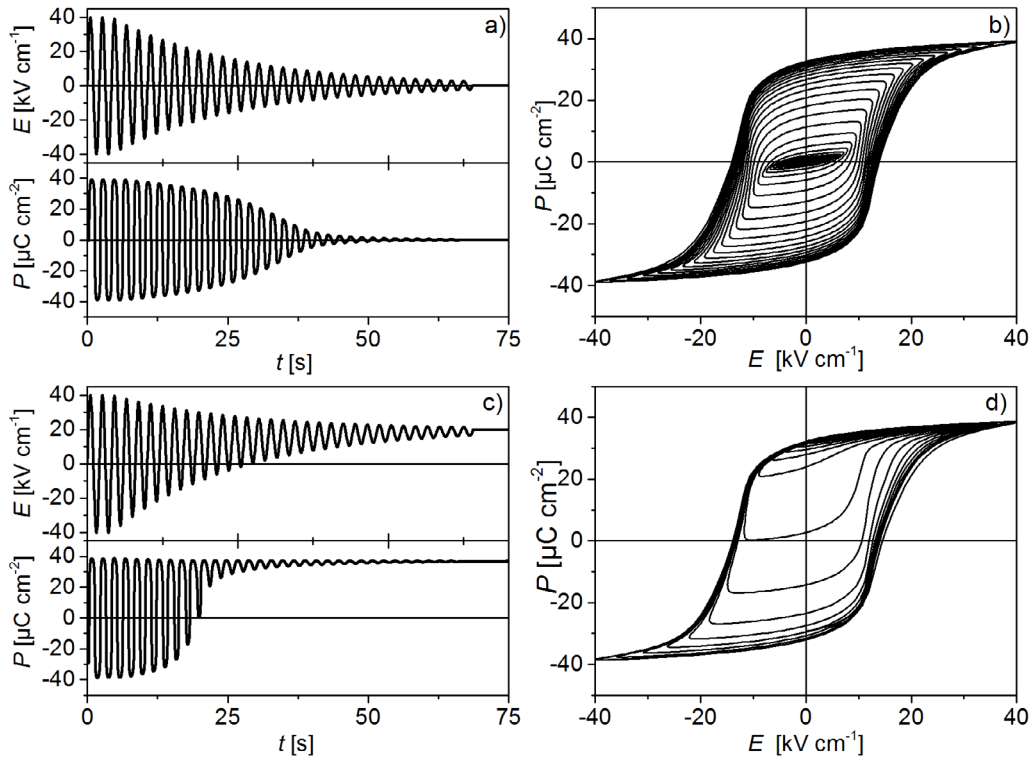


Figure 1. Illustration of the measurement procedure on a doped PZT sample. The applied electric field and measured polarisation as a function of time in a depolarisation procedure for $E_B = 0 \text{ kV cm}^{-1}$ (a) and 20 kV cm^{-1} (c). Macroscopic P - E hysteresis loops for $E_B = 0 \text{ kV cm}^{-1}$ (b) and $E_B = 20 \text{ kV cm}^{-1}$ (d) show the effect of bias field on the depolarisation. This procedure is repeated for several bias fields; each set of (P, E_B) values is plotted to construct the anhysteretic curve shown in figure 2.

PZT (PLZT) [51] and PZT [10, 52, 53]. The hysteresis loop changes shape from a square loop to a slanted loop under compressive stress with a corresponding decrease in remanent polarisation P_r and coercive field E_c , as has been observed previously [10, 51–54]. Between 5 MPa and 50 MPa P_r and E_c decrease by approximately 33% and 10%, respectively. There are a number of intrinsic and extrinsic contributions to the reduction in P_r . One intrinsic contribution is the reduction of the crystal lattice deformation under electric field due to the external stress [10]. Additionally, there are extrinsic contributions due to change in the domain structure caused by compressive stress. The changes to the domain structure depend on the system and may include domain reorientation through non-180° domain walls and stress induced depinning of domain walls [54]. Domain reorientation in the direction perpendicular to the stress leads to a metastable domain configuration and hence to an increase in domain wall motion [55]. This occurs in materials such as BT–1Fe–1.5Nb and hard PZT and results in an observed increase in loss tangent and dielectric constant [54, 56]. In other materials, such as soft La-doped PZT and BT1Fe–0.5Nb, dielectric properties reduce with compressive stress [51, 54] because domain walls are clamped due to stress [54, 57]. The concept of changing the domain configurations via strain has been suggested as a means to enhance piezoelectric properties [58]. The observed reduction in P_r suggests that domains are nucleated more easily under stress. The slanted shape, however, suggests that

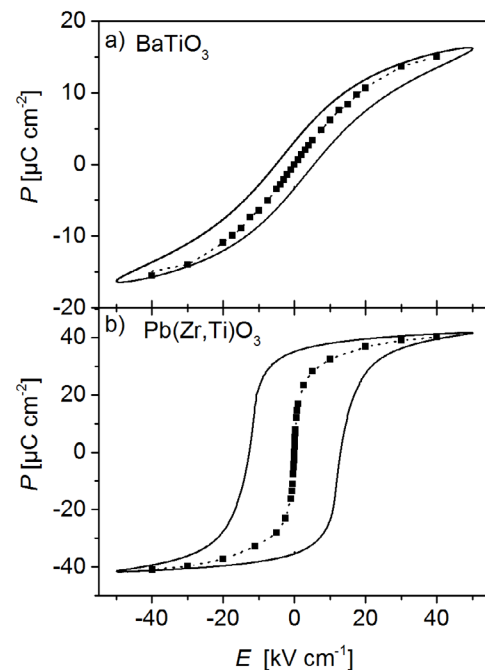


Figure 2. Anhysteretic curves and major loops of (a) BT and (b) doped PZT. A typical major loop of the same material is plotted as a solid line, the data points of the anhysteretic curve are plotted as symbols and the dotted line is a guide to the eye. Each point on the anhysteretic curve was constructed individually following the procedure illustrated in figure 1.

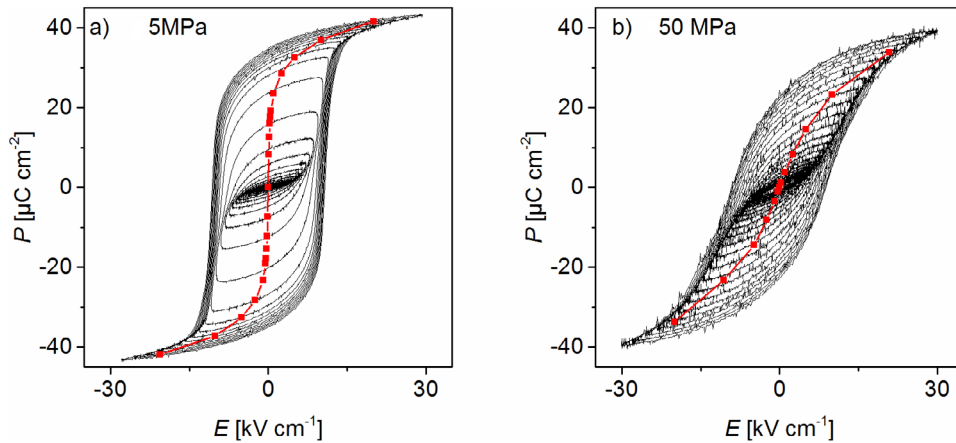


Figure 3. Depolarisation curve and anhysteretic curve of doped PZT obtained under a uniaxial compressive stress (a) 5 MPa and (b) 50 MPa.

there is an obstacle to domain wall motion under compressive stress. The reduction of number of domains participating in the switching process under stress leads to a reduction of energy dissipation and hence the area of the hysteresis loop becomes smaller as observed in other materials [54, 57]. A larger electric field is then necessary to align domains as the compressive stress keeps the ferroelectric domains aligned and away from the stress direction.

Figure 3 shows how the anhysteretic curve also becomes more slanted under stress. In addition to changes in domain processes under stress, the equilibrium case and hence the anhysteretic curve itself changes with stress. This is due to the stress dependent processes not related to defects. The effects observed are a combination of the intrinsic lattice contributions and extrinsic effects dominated by domain wall equilibrium. The relative contribution of intrinsic and extrinsic effects depends on the material and sample microstructure and has rarely been quantified [59, 60]. For PZT films with a thickness $0.5\ \mu\text{m}$ to $3.4\ \mu\text{m}$, for example, the extrinsic contribution of domain wall motion to the dielectric properties was estimated to be 25%–50% and is expected to be higher for thicker samples and larger grains [55]. In the case of single crystal $\text{Pb}(\text{Mg}_{1/3}\text{Nb}_{2/3})\text{O}_3\text{--}0.33\text{PbTiO}_3$ the extrinsic contribution of domain state has been estimated to be 20% from calculations based on experimental data both on as-made samples, and after a polarisation was induced by applying an electric field at elevated temperature [61] (referred to as ‘poled and unpoled samples’ [4, 62]). In the polycrystalline material studied here, the extrinsic contribution from domain wall motion is expected to be significantly higher.

The anhysteretic curve allows separating the different mechanisms involved in ferroelectric behaviour. These effects include intrinsic effects, extrinsic equilibrium effects, i.e. the stable equilibrium of the domain structure, and extrinsic effects responsible for dissipation such as defects. The extrinsic dynamic effects are related to domain wall motion processes and lead to the meta-stable domain configuration while the extrinsic equilibrium effects are static and related to the stable equilibrium domain configuration. The major hysteresis loop

includes all effects, while an anhysteretic curve removes the extrinsic dynamic effects. At low compressive stresses up to 5 MPa, the doped PZT sample shows a factor 10 difference between the equilibrium and non-equilibrium initial susceptibility. At a compressive stress of 50 MPa this difference is reduced to 3.6 fold. This indicates that the contribution of extrinsic dynamic effects is reduced under stress. Further work is necessary to quantify the contribution.

4. Conclusion

The effect of defects on piezoelectric materials under stress is of technological relevance, as electroactive materials are often exposed to elevated stresses during operation. In this study, the anhysteretic polarisation curves of BT and doped PZT were measured for the first time. The comparison of the anhysteretic curve to its major hysteresis loop is a measure of the influence of defects on the material behaviour. The shape of the hysteresis loop is a combination of the anhysteretic contribution and the dissipation mechanism, both of which are sensitive to stress. Comparing both of these gives insights into material behaviour in applications. Future work using computational methods will provide detailed insight into the stress behaviour of ferroelectric materials. Future work including experimental data and calculations of anhysteretic polarisation may help to understand the interplay between ferroelectric domains walls and defects.

Acknowledgments

The authors wish to thank members of the Institute of Glass and Ceramics at Friedrich Alexander University Erlangen Nürnberg (FAU) for technical assistance. FAU received financial support from the Deutsche Forschungsgemeinschaft under WE4972/2. CentraleSuplec received financial support from the Automotive Mechatronics Chair founded by Faurecia, CentraleSuplec and Esigelec.

ORCID iDs

B Kaeswurm  <https://orcid.org/0000-0002-9194-6277>L Daniel  <https://orcid.org/0000-0001-5016-4589>

References

- [1] Bozorth R M 1968 *Ferromagnetism* (Princeton, NJ: Van Nostrand)
- [2] Jiles D C 1998 *Introduction to Magnetism and Magnetic Materials* (London: Chapman and Hall)
- [3] Cullity B D and Graham C 2009 *Introduction to Magnetic Materials* (New York: Wiley)
- [4] Jaffe B, Cook W R and Jaffe H 1971 *Piezoelectric Ceramics* (New York: Academic)
- [5] Pintilie L and Alexe M 2005 Ferroelectric-like hysteresis loop in nonferroelectric systems *Appl. Phys. Lett.* **87** 112903
- [6] Martin B and Kliem H 2005 Electrode effects in solid electrolyte capacitors *J. Appl. Phys.* **98** 074102
- [7] Damjanovic D 2005 *Hysteresis in Piezoelectric and Ferroelectric Materials* vol 3 (Amsterdam: Elsevier)
- [8] Scott J F 2008 Ferroelectrics go bananas *J. Phys.: Condens. Matter* **20** 021001
- [9] Loidl A, Krohns S, Hemberger J and Lunkenheimer P 2008 Bananas go paraelectric *J. Phys.: Condens. Matter* **20** 191001
- [10] Jin L, Li F and Zhang S J 2014 Decoding the fingerprint of ferroelectric loops: comprehension of the material properties and structures *J. Am. Ceram. Soc.* **97** 1–27
- [11] Berger A, Mangin S, McCord J, Hellwig O and Fullerton E E 2010 Cumulative minor loop growth in Co/Pt and Co/Pd multilayers *Phys. Rev. B* **82** 104423
- [12] Roca A G, Vallejo-Fernandez G and O'Grady K 2011 An analysis of minor hysteresis loops of nanoparticles for hyperthermia *IEEE Trans. Magn.* **47** 2878–81
- [13] Barbisio E, Fiorillo F and Ragusa C 2004 Predicting loss in magnetic steels under arbitrary induction waveform and with minor hysteresis loops *IEEE Trans. Magn.* **40** 1810–9
- [14] Lavers J D, Biringer P P and Hollitscher H 1978 Simple method of estimating minor loop hysteresis loss in thin laminations *IEEE Trans. Magn.* **14** 386–8
- [15] Meyer V, Sallèse J M, Fazan P, Bard D and Pecheux F 2003 Modeling the polarization in ferroelectric materials: a novel analytical approach *Solid-State Electron.* **47** 1479–86
- [16] Ricinschi D and Okuyama M 2005 A nucleation-growth model for ferroelectric hysteresis loops with complete and partial switching *J. Eur. Ceram. Soc.* **25** 2357–61
- [17] Kelly P E, O'Grady K, Mayo P I and Chantrell R W 1989 Switching mechanisms in cobalt-phosphorus thin-films *IEEE Trans. Magn.* **25** 3880–3
- [18] Roberts A P, Pike C R and Verosub K L 2000 First-order reversal curve diagrams: a new tool for characterizing the magnetic properties of natural samples *J. Geophys. Res.* **105** 28461–75
- [19] Harrison R G 2009 Physical theory of ferromagnetic first-order return curves *IEEE Trans. Magn.* **45** 1922–39
- [20] Pike C R, Roberts A P and Verosub K L 1999 Characterizing interactions in fine magnetic particle systems using first order reversal curves *J. Appl. Phys.* **85** 6660–7
- [21] Stancu A, Ricinschi D, Mitoseriu L, Postolache P and Okuyama M 2003 First-order reversal curves diagrams for the characterization of ferroelectric switching *Appl. Phys. Lett.* **83** 3767–9
- [22] Fecioru-Morariu M, Ricinschi D, Postolache P, Ciomaga C E, Stancu A and Mitoseriu L 2004 First order reversal curves and hysteresis loops of ferroelectric films described by phenomenological models *J. Optoelectron. Adv. Mater.* **6** 1059–63
- [23] Stoleriu L, Stancu A, Mitoseriu L, Piazza D and Galassi C 2006 Analysis of switching properties of porous ferroelectric ceramics by means of first-order reversal curve diagrams *Phys. Rev. B* **74** 12
- [24] Fujii I, Ugorek M and Trolier-McKinstry S 2010 Grain size effect on the dielectric nonlinearity of BaTiO₃ ceramics *J. Appl. Phys.* **107** 6
- [25] Fujii I, Hong E and Trolier-McKinstry S 2010 Thickness dependence of dielectric nonlinearity of lead zirconate titanate films *IEEE Trans. Ultrason. Ferroelectr. Freq. Control* **57** 1717–23
- [26] Berkowitz A E 1969 *Magnetism and Metallurgy* ed A E Berkowitz and E Kneller (New York: Academic) p 353
- [27] Kneller E 1969 *Magnetism and Metallurgy* ed A E Berkowitz and E Kneller (New York: Academic) p 447
- [28] Wohlfarth E P 1957 The anhysteretic magnetization of permanent magnet alloys *Phil. Mag.* **2** 719–25
- [29] Chantrell R W, Lyberatos A and Wohlfarth E P 1984 Anhysteretic properties of interacting magnetic-tape particles *J. Appl. Phys.* **55** 2223–5
- [30] Chantrell R W and O'Grady K 1992 Magnetic characterization of recording media *J. Phys. D: Appl. Phys.* **25** 1–23
- [31] Hubert O and Daniel L 2008 Multiscale modeling of the magneto-mechanical behavior of grain-oriented silicon steels *J. Magn. Magn. Mater.* **320** 1412–22
- [32] Jiles D C and Atherton D L 1984 Theory of the magnetization process in ferromagnets and its application to the magnetomechanical effect *J. Phys. D: Appl. Phys.* **17** 1265–81
- [33] Jiles D C 1991 Method for deriving information regarding stress from a stressed ferromagnetic material *US Patent Specification* 5,012,189
- [34] Jiles D C 1995 Theory of the magnetomechanical effect *J. Phys. D: Appl. Phys.* **28** 1537–46
- [35] Bertotti G 1998 *Hysteresis in Magnetism For Physicists, Materials Scientists, and Engineers* (New York: Academic)
- [36] Jiles D C and Atherton D L 1986 Theory of ferromagnetic hysteresis *J. Magn. Magn. Mater.* **61** 48–60
- [37] Smith R C and Hom C L 1999 *Proc. SPIE* **3667** 150
- [38] Daniel L, Hall D A and Withers P J 2014 A multiscale model for reversible ferroelectric behaviour of polycrystalline ceramics *Mech. Mater.* **71** 85–100
- [39] Pearson J, Squire P T and Atkinson D 1997 Which anhysteretic magnetization curve? *IEEE Trans. Magn.* **33** 3970–2
- [40] Gould J E and McCaig M 1954 *Proc. Phys. Soc. B* **67** 584
- [41] Johnson H P, Lowrie W and Kent D V 1975 Stability of anhysteretic remanent magnetization in fine and coarse magnetite and maghemite particles *Geophys. J. R. Astron. Soc.* **41** 1–10
- [42] Postnikov V S, Pavlov V S and Turkov S K 1970 Internal friction in ferroelectrics due to interaction of domain boundaries and point defects *J. Phys. Chem. Solids* **31** 1785
- [43] Warren W L, Dimos D, Pike G E, Vanheusden K and Ramesh R 1995 Alignment of defect dipoles in polycrystalline ferroelectrics *Appl. Phys. Lett.* **67** 1689–91
- [44] Shur V, Rummyantsev E, Batchko R, Miller G, Fejer M and Byer R 1999 Physical basis of the domain engineering in the bulk ferroelectrics *Ferroelectrics* **221** 157–67
- [45] Yang T J, Gopalan V, Swart P J and Mohideen U 1999 Direct observation of pinning and bowing of a single ferroelectric domain wall *Phys. Rev. Lett.* **82** 4106–9
- [46] Rojac T, Drnovsek S, Bencan A, Malic B and Damjanovic D 2016 Role of charged defects on the electrical and electromechanical properties of rhombohedral Pb(Zr, Ti)O₃ with oxygen octahedra tilts *Phys. Rev. B* **93** 11

- [47] Lee D, Gopalan V and Phillpot S R 2016 Depinning of the ferroelectric domain wall in congruent LiNbO_3 *Appl. Phys. Lett.* **109** 082905
- [48] Men T L, Thong H C, Li J T, Li M, Zhang J, Zhong V, Luo J, Chu X C, Wang K and Li J F 2017 Domain growth dynamics in $(\text{K}, \text{Na})\text{NbO}_3$ ferroelectric thin films *Ceram. Int.* **43** 9538–42
- [49] Pramanick A, Damjanovic D, Daniels J E, Nino J C and Jones J L 2011 Origins of electro-mechanical coupling in polycrystalline ferroelectrics during subcoercive electrical loading *J. Am. Ceram. Soc.* **94** 293–309
- [50] Böttger U 2005 *Polar Oxides* (New York: Wiley)
- [51] Lynch C S 1996 The effect of uniaxial stress on the electro-mechanical response of 8/65/35 PLZT *Acta Mater.* **44** 4137–48
- [52] Yimnirun R, Laosiritaworn Y and Wongsanmai S 2006 Effect of uniaxial compressive pre-stress on ferroelectric properties of soft PZT ceramics *J. Phys. D: Appl. Phys.* **39** 759–64
- [53] Liu Q D 2011 Investigation into the creeping polarization and strain in PZT-855 under combined mechanical and electrical loadings *Acta Mech.* **220** 1–14
- [54] Unruan M, Sareein T, Tangsritrakul J, Prasertpalichatr S, Ngamjarrojana A, Ananta S and Yimnirun R 2008 Changes in dielectric and ferroelectric properties of $\text{Fe}^{3+}/\text{Nb}^{5+}$ hybrid-doped barium titanate ceramics under compressive stress *J. Appl. Phys.* **104** 124102
- [55] Xu F, Trolier-McKinstry S, Ren W, Xu B M, Xie Z L and Hemker K J 2001 Domain wall motion and its contribution to the dielectric and piezoelectric properties of lead zirconate titanate films *J. Appl. Phys.* **89** 1336–48
- [56] Zhang Q M, Zhao J Z, Uchino K and Zheng J H 1997 Change of the weak-field properties of $\text{Pb}(\text{ZrTi})\text{O}_3$ piezoceramics with compressive uniaxial stresses and its links to the effect of dopants on the stability of the polarizations in the materials *J. Mater. Res.* **12** 226–34
- [57] Zhou D Y, Wang Z G and Kamlah M 2005 Experimental investigation of domain switching criterion for soft lead zirconate titanate piezoceramics under coaxial proportional electromechanical loading *J. Appl. Phys.* **97** 84105
- [58] Schmidbauer M, Braun D, Markurt T, Hanke M and Schwarzkopf J 2017 Strain engineering of monoclinic domains in $\text{K}_x\text{Na}_{1-x}\text{NbO}_3$ epitaxial layers: a pathway to enhanced piezoelectric properties *Nanotechnology* **28** 7
- [59] Schader F H, Rossetti G A, Luo J and Webber K G 2017 Piezoelectric and ferroelectric properties of $\langle 001 \rangle_c$ $\text{Pb}(\text{In}_{1/2}\text{Nb}_{1/2})\text{O}_3$ - $\text{Pb}(\text{Mg}_{1/3}\text{Nb}_{2/3})\text{O}_3$ - PbTiO_3 single crystals under combined thermal and mechanical loading *Acta Mater.* **126** 174–81
- [60] Damjanovic D and Demartin M 1996 The Rayleigh law in piezoelectric ceramics *J. Phys. D: Appl. Phys.* **29** 2057–60
- [61] Damjanovic D, Budimir M, Davis M and Setter N 2003 Monodomain versus polydomain piezoelectric response of $0.67\text{Pb}(\text{Mg}_{1/3}\text{Nb}_{2/3})\text{O}_3$ - 0.33PbTiO_3 single crystals along nonpolar directions *Appl. Phys. Lett.* **83** 527–9
- [62] American National Standard 1986 ANSI/IEEE Std 180-1986 IEEE Standard Definitions of Primary Ferroelectric Terms (Revision of IEEE Std 180-1962)